

Temperature difference in close-spaced sublimation (CSS) growth of CdTe thin film on ultra-thin glass substrate

C. Doroody^a, K.S. Rahman^{b,*}, S.F. Abdullah^c, M.N. Harif^a, H.N. Rosly^a, S.K. Tiong^c, N. Amin^{c,*}

^a College of Engineering, Universiti Tenaga Nasional (@The Energy University), Jalan IKRAM-UNITEN, 43000 Kajang, Selangor, Malaysia

^b Solar Energy Research Institute, Universiti Kebangsaan Malaysia, 43600 Bangi, Selangor, Malaysia

^c Institute of Sustainable Energy, Universiti Tenaga Nasional (@The Energy University), Jalan IKRAM-UNITEN, 43000 Kajang, Selangor, Malaysia

ARTICLE INFO

Keywords:

Cadmium telluride
Thin film
Close-spaced sublimation
Deposition temperature
Ultra-thin glass substrate

ABSTRACT

In this study, cadmium telluride (CdTe) thin films were grown for the first time ever on ultra-thin (100 μm) Schott D263T glass substrates via high temperature deposition process namely close-spaced sublimation (CSS). CdTe thin films were deposited under different source and substrate temperatures ranging from 500 $^{\circ}\text{C}$ to 700 $^{\circ}\text{C}$ to investigate the influence of deposition temperature on the properties of CdTe thin films grown on ultra-thin Schott glass substrates. X-ray diffraction (XRD) analysis illustrated cubic CdTe structure with a sharp peak at (111) orientation. The scanning electron microscope (SEM) study elucidated that the grain growth and surface morphology were highly dependent on the deposition temperature. UV-Vis results showed approximate optical band gap range of 1.61–1.66 eV. Carrier concentration and resistivity were found in the order of 10^{13} cm^{-3} and $10^5\ \Omega\text{-cm}$, respectively. Structural and opto-electronic characteristics were optimized for the best temperature range to be used for CdTe film deposition in CSS growth. Optimum conditions for CdTe film growth on ultra-thin (100 μm) substrate were found in the range of 500 $^{\circ}\text{C}$ –600 $^{\circ}\text{C}$ for substrate and source temperature.

Introduction

Presently, thin film solar cells based on CdTe absorbers are a leading photovoltaic technology producing electricity at costs competitive with conventional fuels [1]. High absorption coefficient ($> 10^4\text{ cm}^{-1}$), nearly ideal direct band gap (1.45 eV) and ease of synthesis enable the light to be absorbed and converted to electricity in several micrometre thick CdTe layers, that can be deposited on a range of substrates, including glass, metal foils, polymers and ultra-thin glass for standard, lightweight and flexible design [2,3]. Lightness and flexibility offer lower production cost, compatible designs as well as thermal stability up to the optimal CdTe growth temperature ($\sim 700\text{ }^{\circ}\text{C}$) using ultra-thin glass substrates [4]. However, operational stresses and essential lifetime also need to be considered. Moreover, the substrate conformation confers the solar cells to be combined effortlessly with other devices, offering smooth maintenance process [5]. Early studies on flexible glass substrates were mainly focused on low temperature process. Therefore, high temperature range applicable for CdTe flexible solar cells is poorly understood. Thin film solar cells are just a few micrometres thick, facilitating higher flexibility compared to Silicon cells. However, bendability is restricted to a critical radius [6]. Most of the transparent polymers or plastic suffers from moisture, chemical penetration and

serious inflection through the general processing temperature ($> 400\text{ }^{\circ}\text{C}$) [7]. Also, most of the highest efficiency CdTe thin film solar cells are grown using high temperatures ($> 500\text{ }^{\circ}\text{C}$) process such as CSS and harsh chemical environments (Cl or Se ambient), which are incompatible with some substrates [8]. Thus, the possible choice as a flexible and efficient substrate which is highly transparent and can withstand high temperature ($> 650\text{ }^{\circ}\text{C}$) is ultra-thin glass substrate [9]. Meanwhile, it has been proved that p–n homojunction structure is unstable due to the aging behaviour of dopants in CdTe films and bulk single crystals [10]. Also, it is tough to fabricate shallow p–n junctions with highly conducting surface layers, that may result in substantial losses and difficult optimization [11]. As CdS/CdTe hetero-junction has decent rectification properties, CdTe is presumed to be p-type to form a p–n junction rectifying device with its n-CdS partner [12]. The suggested thickness of CdS layer is around 100 nm to assure the transmittance and suitable morphology [13]. In 1984, 10% efficiency for CdTe thin film solar cells was surpassed at Kodak laboratories, using the CSS method [14]. In 1993, 15.8% efficiency was achieved by a researcher from the South Florida University that used the CSS again to deposit CdTe films on borosilicate glass at about 650 $^{\circ}\text{C}$ [15]. Seven years later, a group from National Renewable Energy Laboratory (NREL), achieved 16.5% efficiency [16]. From 2013 to 2016, significant

* Corresponding authors.

E-mail addresses: sajed_cuet_eee@yahoo.com (K.S. Rahman), nowshad@uniten.edu.my (N. Amin).

<https://doi.org/10.1016/j.rinp.2020.103213>

Received 2 April 2020; Received in revised form 20 June 2020; Accepted 22 June 2020

Available online 26 June 2020

2211-3797/ © 2020 Published by Elsevier B.V. This is an open access article under the CC BY-NC-ND license (<http://creativecommons.org/licenses/by-nc-nd/4.0/>).

increment in efficiency from 16.5% to 22.1% was attained for CdTe thin film solar cells [17].

Conventionally, CdTe thin film solar cells are fabricated on stiff glass substrates [18,19]. But the devices on stiff substrates have the disadvantage of weight compared to the ultra-thin and flexible glass substrates [19]. On the other hand, the devices on flexible glass substrates can offer the same high transparency in a much lower weight and will make the full cell to become portable and compatible to be fixed on any type of surface area. Schott Solar originated from the earliest PV activities in Germany, based mainly on multi crystalline silicon cells and Schott D263T series as an ultra-thin flexible glass substrate [20]. Schott D263T has already been successfully demonstrated in the lightweight X-ray optics for space-borne application [21], organic light emitting devices (OLED) [22], flexible polymer light emitting devices (PLED) [23] and photodetectors [24]. Hence, the development and characterization of CdTe thin film grown by CSS on ultra-thin D263T glass substrates are interesting. More than ten deposition methods have been utilized so far to grow CdTe thin film such as magnetron sputtering [25], close-spaced sublimation [26,27], vapor transport deposition (VTD) [28] and screen print deposition [28]. CSS is a leading method for CdTe thin film deposition due to the ease of use and cost-effectivity [29,30]. This system is advantageous compared to competing coating methods for its smart utilization of materials, short substrate-source distance (~1 mm) and high deposition rate in shorter time [31]. Some reports are available regarding the analysis of CdTe thin film grown by CSS [32], but practically there are no published reports regarding the characterization of CdTe thin films developed on Schott ultra-thin (100 μm) glass substrates via CSS technique in a diverse temperature interval. The growth rate of CSS method depends on the source-substrate distance, source-substrate temperature, the pressure, deposition time and temperature and gas composition in the deposition chamber [33]. Therefore, the foremost significance of this study is to inspect the growth of CdTe thin films on ultra-thin (100 μm) Schott glass substrate by CSS as well as to investigate the influence of deposition temperatures on CdTe thin films.

Experimental details

Thin film growth by CSS

Initially, ultra-thin (100 μm) Schott glass substrates were pre-cut with a dimension of 3 cm \times 3 cm (Fig. 1a). The glass substrates were ultrasonically cleaned with a sequence of (Methanol-Acetone-Methanol-DI water). After cleaning, samples were dried by a jet stream of industrial N_2 gas. Primarily, CdS thin films were grown by Radio Frequency (RF) sputtering technique using 5 cm diameter target with a target-substrate distance of about 13 cm. Deposition chamber was vacuumed to about 1×10^{-5} Torr and all runs were performed at room temperature. An operating pressure of 2.8×10^{-2} Torr, RF power of

Table 1

Deposition condition for CSS grown CdTe films.

Parameter	Condition
Substrate Temperature	500 °C–650 °C
Source Temperature	600 °C–700 °C
Deposition Pressure	1–1.5 Torr (Ar ambient)
Source-substrate Distance	1 mm
Deposition Time	10 min

40 W and deposition time of 10 mins were utilized to yield 150 nm thick sputtered CdS (Fig. 1b) [61]. Subsequently, CdTe films were grown by CSS method (Fig. 1c). The CSS system used in this study, includes quartz tube reinforced by a reactor, halogen lamps as a heat source, thermocouples, and PID controllers to control the temperatures of the source and the substrate. The distance between the source and the substrate was 1 mm. Usually, lower distance between the source and substrate reduces the loss probability of mass transport during sublimation [3].

The details of the used CSS system in this experiment can be found elsewhere [33,34]. CSS is a technique in which the solid is transformed into vapor at high temperature in a vacuum. The deposition on the substrate will get into an equilibrium state if the source and the substrate temperatures are the same, thus the film thickness will stop increasing [35]. Accordingly, in this study, temperature was varied for both the source and the substrate during the film growth. Deposition time was kept constant at 10 mins in all temperature variations. Table 1 shows the deposition parameters of CdTe film grown via CSS.

CdTe thin film characterization

Structural properties and preferred crystallographic orientation were characterized by Shimadzu XRD-6000 X-ray diffractometer using $\text{Cu K}\alpha$ radiation wavelength ($\lambda = 1.5406 \text{ \AA}$) with a step size of 0.02° in the 2theta range from 20 to 60° at room temperature. The grain size, surface morphology, compositional analysis and thickness were studied with a Hitachi SU1510 scanning electron microscope (SEM) which was operated at an accelerating voltage of 15 kV and equipped with Thermo Fisher Scientific UltraDry EDS Detector. Optical measurements were taken in the wavelength range of 200–1000 nm using the Perkin-Elmer-Lambda-35 UV-vis spectrophotometer. The electrical parameters were measured by ECOPIA HMS-3000 Hall Effect measurement with a magnetic field of 0.57 T and probe current of 45 nA for all the samples.

Results and discussion

It has been already recognized that the high efficiencies attained from CSS CdTe films have been ascribed to the high substrate temperature. Basically, high temperature encourages the interface reaction

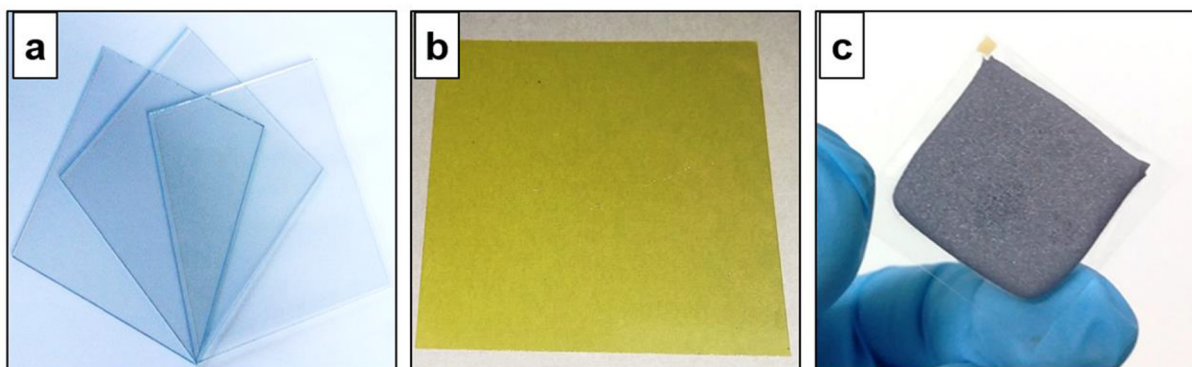


Fig. 1. (a) Ultra-thin Schott glass substrates before deposition (b) sputtered CdS thin film and (c) CdTe thin film grown by CSS.

Table 2
Simplified sample name for different source and substrate temperatures.

Sample ID#	Source Temperature (°C)	Substrate Temperature (°C)
A	600	500
B	600	550
C	625	575
D	650	600
E	675	625
F	700	650

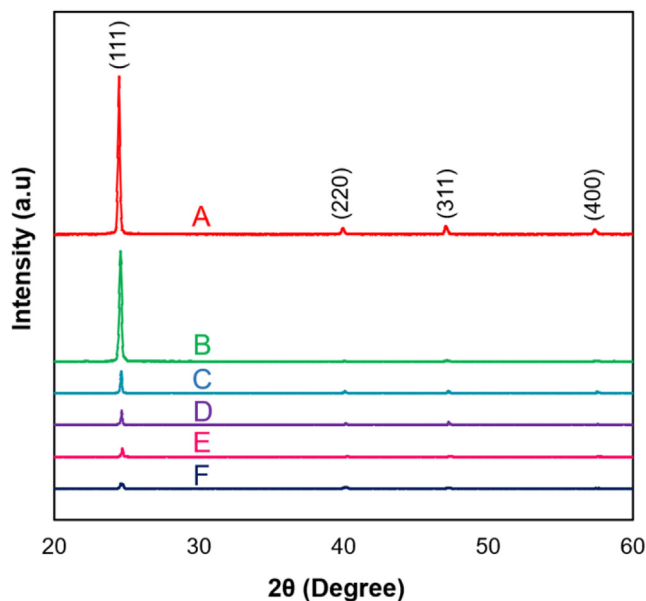


Fig. 2. XRD patterns of CdTe thin films deposited at different source-substrate temperatures.

between the CdS and CdTe. In this study, different source and substrate temperatures have been highlighted to attain the optimum CSS growth process for uniform, pinhole free and thin CdTe films. Table 2 specifies the simplified sample ID for different source and substrate temperatures of CSS grown CdTe thin films.

Structural characterization

The XRD technique was employed to study the crystallinity and phase of CdTe thin films. The XRD patterns in Fig. 2 presents the strong preferential diffraction peak located at $2\theta = 24.60^\circ$ corresponding to (111) reflection plane confirming a cubic zinc blende structure [60]. XRD peaks confirm that the pattern is dominated by (111) plane and the other three CdTe peaks, (220), (311) and (400) are having very weak intensity compared to (111). Typically, diversity in peak intensities may be related to the various scattering intensity of crystal components or lattice alignment or because of the discrepancies in crystallite size. Also, it may happen due to the influence of CdS layer interdiffusion in CdTe during high temperature deposition or the roughness of substrate. Therefore, strengths of (111) peak differ for high deposition temperatures that are in accord with the XRD results published previously [36]. High intensity of (111) plane confers that 500°C to 600°C temperature range leads to the plane orientation to form a more crystalline structure. There is no existence of pure cadmium, tellurium or any other oxides formation in XRD patterns. In addition, diffraction pattern follows the $\text{CdS}_x\text{Te}_{1-x}$, where $x = 0.2$ to 0.4 according to the report obtained by Ohata et al. [38], where the value of lattice constant in $\text{CdS}_x\text{Te}_{1-x}$ at $x = 0.4$ is about 6.24 \AA .

XRD diffraction peaks at $2\theta = 24.60^\circ, 39.49^\circ, 46.49^\circ$ and 57.5° corresponding to planes (111), (220), (311) and (400), respectively,

Table 3
Calculated structural parameters of CdTe thin films.

Sample ID#	hkl	β (deg)	d_{hkl} (nm)	a (Å)	D (nm)	ϵ ($\times 10^{-3}$)	δ ($\times 10^6$) cm^{-2}
A	(111)	0.24	0.36	6.28	25.39	4.80	1.55
B	(111)	0.36	0.36	6.26	16.93	7.19	3.48
C	(111)	0.34	0.36	6.26	17.92	6.39	2.75
D	(111)	0.44	0.36	6.26	13.25	10.39	7.27
E	(111)	0.38	0.36	6.24	16.04	7.96	4.30
F	(111)	0.40	0.36	6.26	15.23	8.38	5.75

are well-indexed with the JCPDS Card No. 03-065-1046 [60]. By using Bragg's law [$d_{(hkl)} = (\lambda/2) \text{cosec}\theta$] and Vegard's law [$a_{\text{cubic}} = d_{hkl} (h^2 + k^2 + l^2)^{1/2}$], lattice constant 'a' is calculated [25,42]. The average crystallite grain size (D) is calculated using the Scherrer's formula [$D = 0.9\lambda/\beta \text{cosec}\theta$] [37]. The microstrain (ϵ) is obtained from the equation [$\epsilon = \beta/4 \tan\theta$] [39]. To calculate dislocation density, Williamson and Smallman's relation [$\delta = n/D^2$] is used [39]. Here, D is the grain size or the average diameter of every crystal orientation in polycrystalline material and grain size enlargement using high temperature reduces the lattice mismatch within specific temperature range [40]. The calculated structural parameters are shown in Table 3. The lattice constant is unaffected by different temperatures and found to be 0.63 nm . Fig. 3 depicts the variation of FWHM and crystallite size for various temperatures. Estimated crystallite grain size ranges from 13 nm to 25 nm for (111) plane.

Fig. 4 shows increased dislocation density and microstrain at temperatures higher than 600°C which may be due to a higher lattice misalignment and imperfections. Therefore, it is apparent that the best deposition temperature range for CdTe thin film deposition is about 500°C to 600°C . The rise in strain and dislocation with increasing temperature can be illustrated by the considerable increment in the assembling disorder of films [41]. The maximum microstrain of 10.4×10^{-3} and dislocation density of $7.27 \times 10^6 \text{ cm}^{-2}$ are obtained for the sample D. Stress during deposition can lead to fluctuations in the diffraction results. Lowest strain associates to sample A and B with high crystallinity that is needed in the high efficiency cell fabrication. The dislocation density is detected to increase with the deposition temperature because of degraded crystallite orientation. This leads to the establishment of lower quality films with nonuniform crystallinity for high growth temperatures and results are in compliance with the paper published earlier [43].

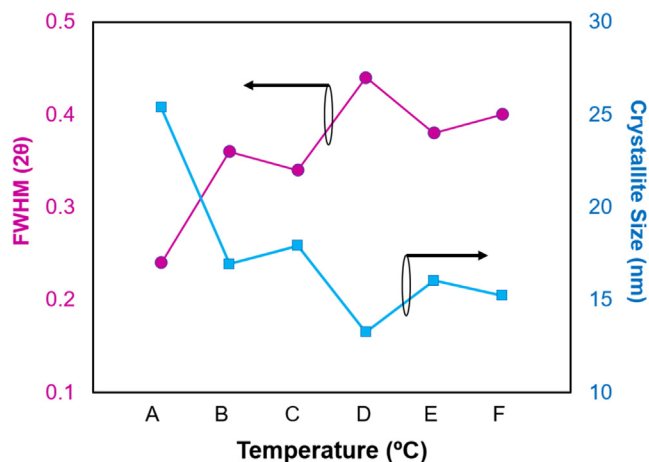


Fig. 3. Variation of FWHM and crystallite size with temperature.

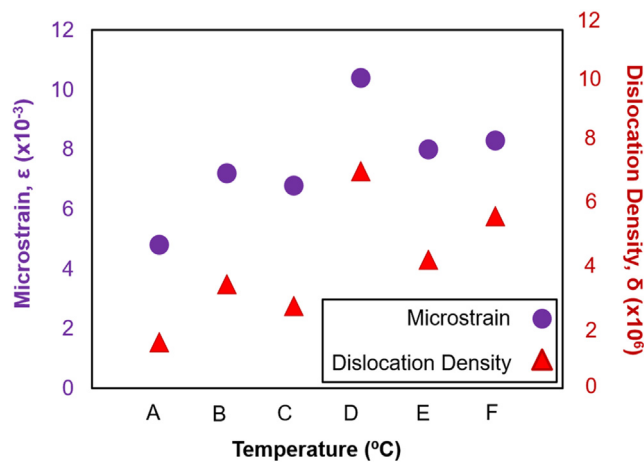


Fig. 4. Microstrain and dislocation density variations with temperature.

Surface morphological and compositional properties

Fig. 5 presents the SEM micrographs for CdTe films deposited at substrate/source temperature range from 500 °C to 700 °C. From the SEM morphology images, it is obvious that the grain size is directly correlated to temperature. The SEM images could show the coalition of small crystallites into large grain that is hard to be resolved to individual crystallite [30]. For high temperature, grain size enlarges to an average of 20 μm . The bulk structure and the average grain size are initially correlated to the deposition temperatures as a function of thickness as evident from the SEM results.

In order to investigate any possible interdiffusion from glass substances or sulfur into the CdTe layer, the energy-dispersive X-ray spectroscopy (EDX) spectrogram of CdTe thin films is presented in Fig. 6. The EDX spectrogram reveals the presence of identical Cd and Te dominance in all the samples with nearly 1:1 ratio and verifies the stability of CdTe thin film through different temperatures. Further increase in the temperature may lead to the glass substrate deformation, as well as sulfur/indium interdiffusion in absorber layer.

Fig. 7 specifies the changes in measured thickness and grain size with the deposition temperatures of CdTe thin film. The thickness increases from 6 μm to 45 μm . The increment in thickness becomes faster with the increase in deposition temperature higher than 600 °C. As the deposition time (10 min) and pressure (below 5 Torr) are kept constant during CdTe film growth, the growth rate is sublimation limited and has a positive exponential dependence on temperature while increasing the source temperature from 600 °C to 700 °C, and substrate temperature from 500 °C to 650 °C. Nevertheless, stress level and thermal expansion coefficient linked to the glass substrate will cause undesirable diffusion of sulfur and glass elements such as indium in CdTe layer for $T_{\text{substrate}} \geq 600$ °C, and substrate deformation will happen which results in the nonuniform deposition [1]. Grain size is found below 6 μm for the samples deposited at 500 °C and is gradually increases to 20 μm for the samples sublimated at (≥ 600 °C). As a result of high temperature deposition, CdS diffusion is controlled by reducing the number of possible diffusion pathways (pinholes), which are grain boundaries and crystallographic defects in CdS/CdTe films. CSS deposition at $T > 500$ °C enhances grain size, reduces crystallographic defects, and retards diffusion of CdS into CdTe [44]. Also, high concentrations of inherent point defects happen through the sublimation because of the diffusion effectively stops at temperature of 500 °C or even higher [45]. Moreover, the bulk thickness is appeared to increase with temperature although the crystal structure shows better crystallinity for sample A and B as detected from the structural studies. Also, grain size is blasted within the high temperature range over 600 °C. The results are well consistent with XRD analysis. A further rise in temperatures leads to

higher deposition rates and larger grains as anticipated [46]. However, source plates display poor consistency with the existence of blasted particles [47]. Moreover, in case of temperature above 700 °C, the characteristics of CdTe may change due to the phase change in CdTe and Te re-evaporation and CdTe re-sublimation will probably be much higher which can change the composition affecting the physical properties of the CdTe absorber layer [1].

There are numerous approaches to compute diffraction peak profile using diffraction width, such as Scherrer formula, Williamson-Hall plot, etc. However, each of them differs in the basis, results and order of magnitudes which make it impossible to compare them directly or make an exact result for grain size using any of the available means. Overall, all existing procedures are capable to provide some estimates of exact grain size [30]. XRD calculate the size of the crystalline domains while SEM exhibits physical grains. A single grain can comprise several domains with dissimilar orientations. Therefore, the size measured by SEM will be always larger or, in case of the perfect grains, equal to that calculated by XRD. Crystallite size denotes the measurement of the size of coherently diffracting regions which is typically calculated from the XRD pattern using the Scherrer equation. In the Scherrer formula, many assumptions are being considered which could be dissimilar for the actual samples. It presumes that all crystallites have the identical shape and size although the shape of crystallites is typically asymmetrical. In contrast, grains are volumes inside crystalline materials with a definite orientation. Grain size generally means the average diameter of the individual crystal orientations found in polycrystalline materials. During the thin film growth process, smaller crystallites become bigger due to kinetics. Consequently, in the most possible scenario, the grain is larger than a crystallite. Crystallite size is equal to grain size if the grain is perfectly single crystallite [30]. Grain size and morphology are commonly determined by SEM (but not XRD). The grain size measured from SEM analysis could be the combination of small crystallites into one large grain made of several crystallites and it is occasionally tough to resolve individual crystallite from SEM [30]. Therefore, grain size measured from SEM is an average value whereas the Scherrer formula calculates the crystallite size using the diffraction information from a single plane at a specific 2θ and FWHM value [30]. Overall, XRD technique offers the information of the crystallite size present in the grains while the microscopic investigation via SEM provides the average grain size of the material. Since grain encompasses many crystallites, the crystallite size and grain size are not same.

Optical characterization

Optical properties of CdTe films have been derived from the absorbance spectra of the films using UV-Vis spectrophotometer. The energy band gap, E_g and the nature of transition are analysed by the equation $[\alpha h\nu = A (h\nu - E_g)^{1/2}]$ [30]. Fig. 8 displays the Tauc graph to compute the direct energy band gap. Grain uniformity of the substrate surface affect the optical absorbance and band gap allocation of films. The direct band gap is attained and analysed by drawing a straight-line through the portion of graph to zero absorption coefficients. The band gap is assessed by generalizing the straight line on the Tauc plot for zero absorption coefficients.

The nature of the Tauc plot confirms CdTe as a direct band gap semiconductor. The energy band gap is attained to be in the range of 1.61–1.66 eV and the change in band gap is related to altered Cd stoichiometry as well as change in crystallinity [48]. Furthermore, changes in the absorption shift and carrier concentration will lead to the band gap changes, which is clarified by the Burstein–Moss effect [49]. The Burstein–Moss effect refers to the fermi level position respecting to conduction band that directs to energy band expansion [49]. Thus, the shrinkage effect is leading, and band gap is reduced slightly with the increment of temperature.

As evident in EDX compositional ratio, there is no sign of interdiffusion or excess Cd intermixing involvement which affect the band

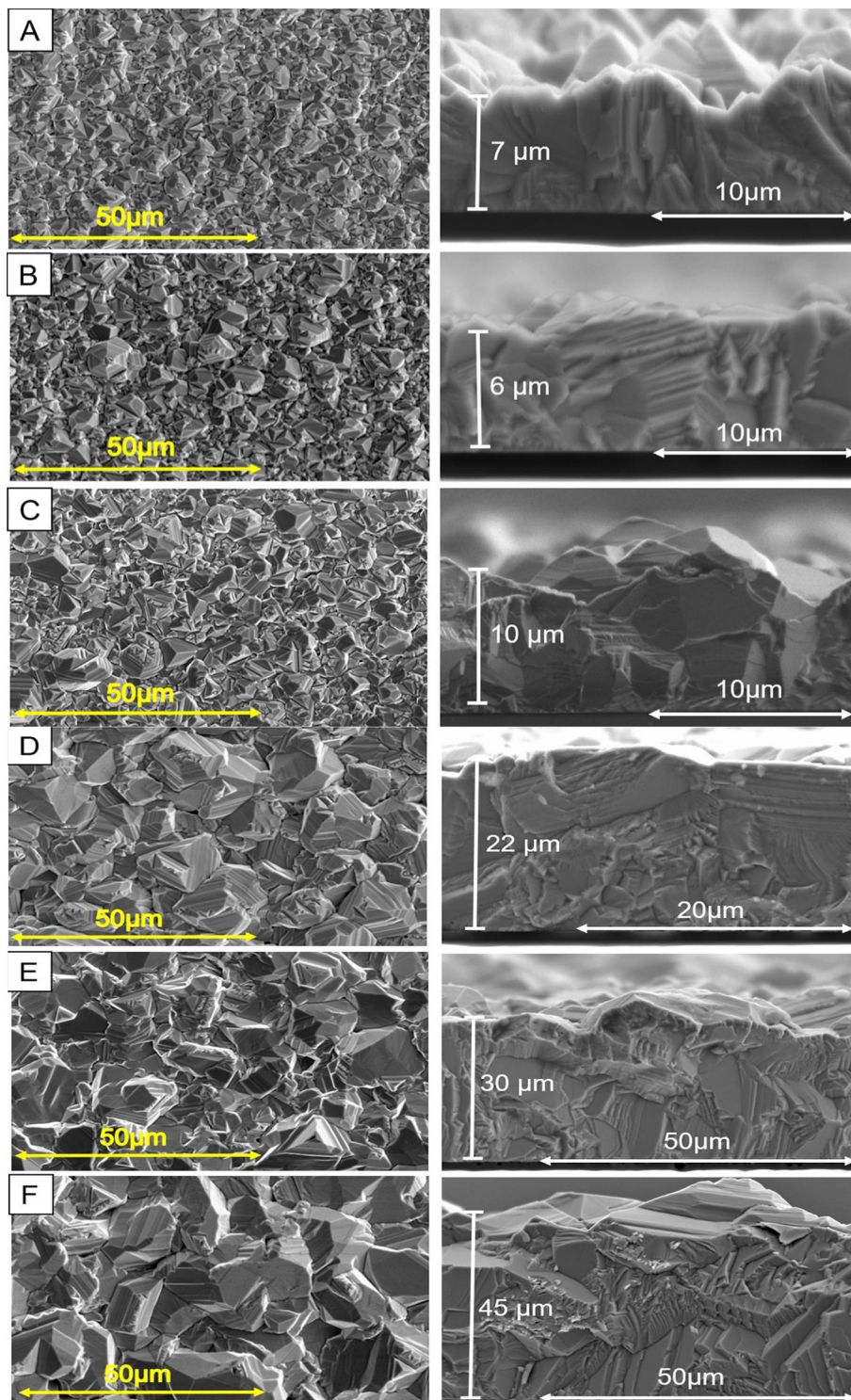


Fig. 5. SEM surface morphology and cross section images of CdTe thin films.

gap. In case of compound semiconductors, the optical band gap can be affected by the stoichiometric deviations, dislocation density, grain boundaries disorder, quantum size effect and change in preferred orientation [50]. The high optical energy band gap of as-grown thin films may be due to the existence of dislocations which discloses that the dislocations are detached by a distance larger than the inter-atomic distance [51]. Chander et al. stated that as deposited CdTe thin film without treatment had energy band gap range of 1.6–1.78 eV that might be due to aforesaid deviation phenomenon located in inter-atomic scales [51]. This high band gap value could be shifted to

approximately 1.5 eV through post-deposition treatment [52]. Decline in band gap after annealing or CdCl₂ treatment may be due to reduction in dislocation density, increase in grain size and more realignment in orientation leading to enhanced crystallinity [51,53]. The band gap may also be declined due to loss of cadmium in CdTe films resulting the formation of shallow acceptor levels [54]. Band gap reduction through treatment may also be due to the variation in plasma frequency which could be ascribed to the modification in film carrier density and mobility [55]. Strong interaction between the substrate and vapor atoms on treated samples could be another factor of band gap reduction [55].

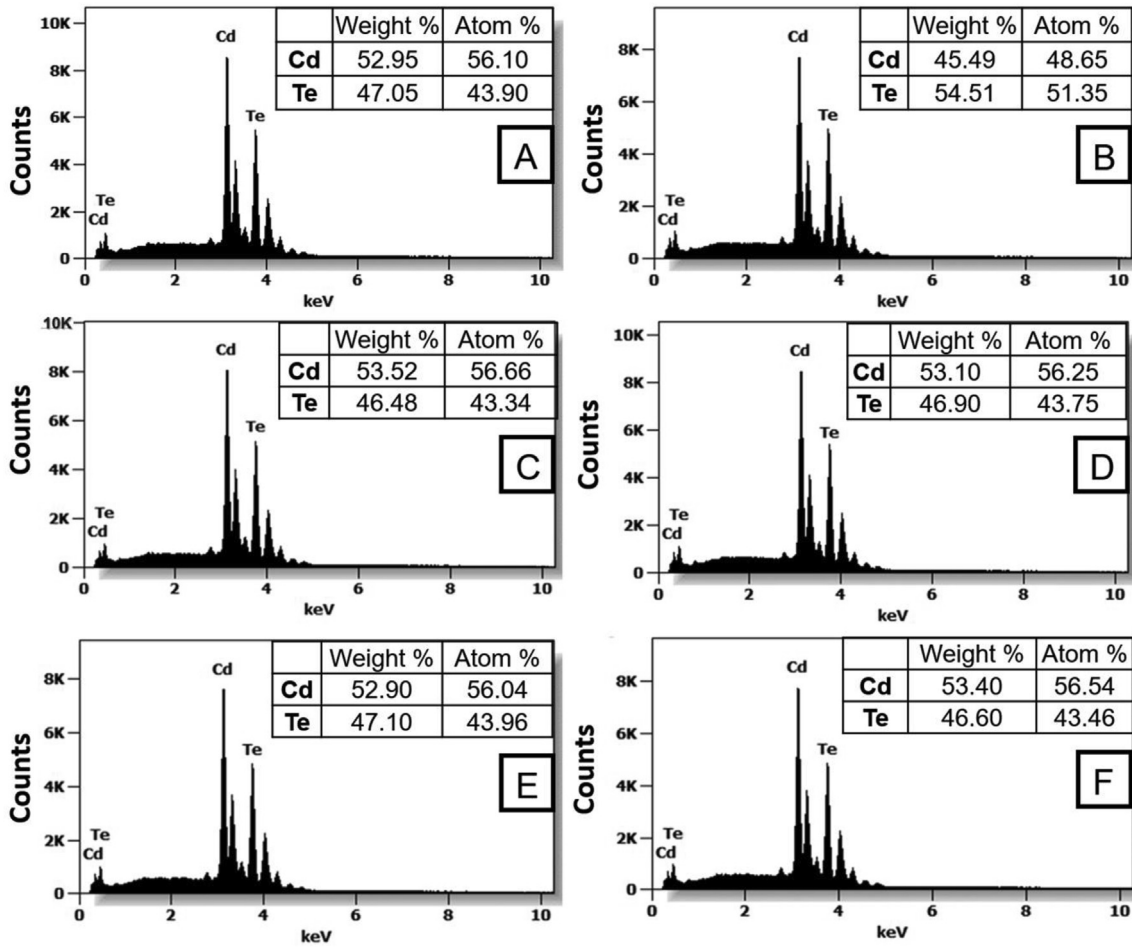


Fig. 6. EDX spectrogram of CdTe thin films with compositional ratio.

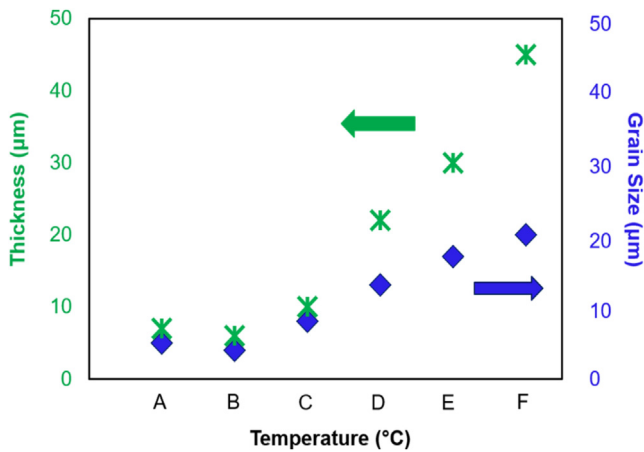


Fig. 7. Thickness and grain size variation for CSS deposited CdTe thin films.

A study by Kokate et al. [56] reported that the direct optical band gap of CdTe thin film was approximately 1.65 eV before treatment and 1.5 eV after treatment. Shaaban et al. [57] and Khairnar et al. [58] stated the thickness-dependent energy band gap of treated CdTe thin films in the range 1.45–1.55 eV.

Electrical properties

In order to measure the electrical parameters by Hall effect measurement, four electrode (1 cm × 1 cm) contacts were formed using

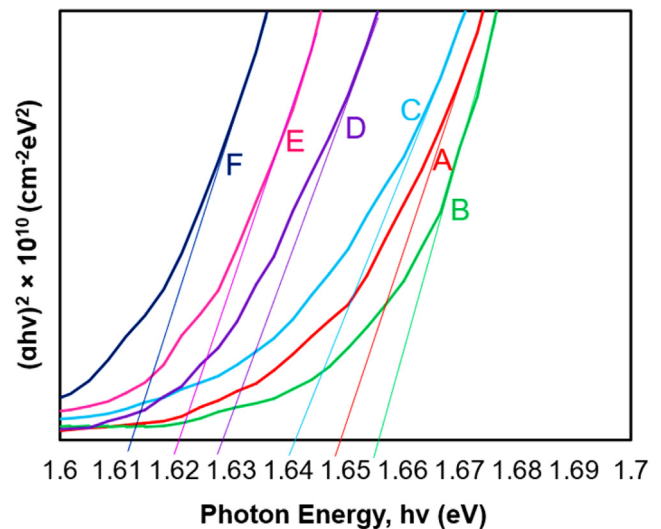


Fig. 8. Plot of $(ahv)^2$ versus photon energy ($h\nu$) for the band gap calculation of CdTe thin films.

adhesive silver conductive paste in each corner of the sample. The magnetic field was applied vertically to the sample surface and the magnitude and polarity were interchanged periodically, while a direct current was passed across the sample by means of one diagonal pair of the four gold electrodes allied to a current source. Then, by a frequency response analyser (HMS-3000), alternating Hall voltage induced

Table 4
Electrical parameters of CdTe thin films.

Sample	Carrier Concentration [$\times 10^{13}$] ($/\text{cm}^3$)	Mobility (cm^2/Vs)	Resistivity [$\times 10^5$] ($\Omega\text{-cm}$)
A	2.05	10	1.30
B	1.88	7	1.07
C	1.06	9	2.02
D	0.59	5	4.34
E	0.14	6	6.15
F	0.20	7	9.10

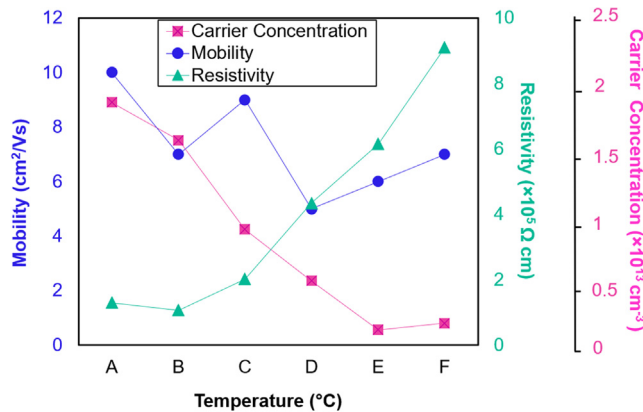


Fig. 9. Carrier concentration, resistivity and mobility variation with temperature.

synchronously with the AC magnetic field was detected via the other pair of electrodes. The detection limit of the Hall voltage has significantly improved by following this method. Table 4 presents the electrical parameters of CdTe film. The grown films show p-type conductivity with carrier concentration ranging from $0.14 \times 10^{13} \text{ cm}^{-3}$ to $2.05 \times 10^{13} \text{ cm}^{-3}$. The highest mobility has been achieved for sample A while the lowest resistivity has been attained from the sample B. The conductivity values for different temperature vary by the crystal structural defects and surface chemical reaction [24]. The relation of carrier concentration, mobility, and resistivity are presented as $[\sigma = qn\mu_n]$ and $[\sigma = 1/\rho]$.

The mobility reduces with the rising temperature. After sample A, the carrier concentration lessens by the excess in temperature. The values presented here could be resulted from the rise in the dislocation density, as in Fig. 4, which shows carrier scattering and slight mobility reduction. The resistivity in the range of $10^5 \Omega\text{-cm}$ is showing slight changes regarding the deposition conditions, in accordance with the earlier study [59]. Fig. 9 presents the electrical properties variation of CdTe thin films for different temperatures.

The carrier concentration is found in the order of 10^{13} cm^{-3} for all the deposited samples. Perception and controlling the carrier concentration of CdTe polycrystalline thin films have been extremely challenging, as it is tough to dope high concentration owing to self-compensation from intrinsic defects form e.g: vacancies (V_{Cd} , V_{Te}), interstitial defects (Cd_i , Te_i) and grain boundaries [30,40]. Consequently, the measured carrier concentration is low which is one of the key challenges to improve CdTe solar cells performance. Therefore, it is confirmed that the discrepancy of deposition temperature has major impact on film properties.

Conclusion

Impact of temperature on the structural and opto-electronic properties of CdTe thin films have been scrutinized elaborately in this study. From the analysis, it has been found that the growth rate is a factor of temperature difference between the source and the substrate. High

temperature accelerates the growth rate and grain size, however, at the compromise of film quality. The XRD analysis illustrates that CdTe thin films show a cubic zinc blende structure preferentially oriented along (111) plane. The average grain size has been obtained in the range of 4–20 μm and the EDX spectra discloses Cd and Te dominance with approximately 1:1 ratio. The optical band gap is found in the range of 1.61–1.66 eV. The highest carrier concentration and mobility are obtained for the sample deposited at a temperature range of 500 $^\circ\text{C}$ –600 $^\circ\text{C}$. Optimized parameters are obtained using 500 $^\circ\text{C}$ to 600 $^\circ\text{C}$ temperature range for CSS deposition. Therefore, all the characterization results of CdTe thin films grown on ultra-thin (100 μm) Schott glass substrates suggest their potential to be used as the absorber layer to fabricate CdS/CdTe thin films solar cells.

CRedit authorship contribution statement

C. Doroody: Data curation, Methodology, Writing - original draft, Software, Formal analysis. **K.S. Rahman:** Conceptualization, Methodology, Investigation, Project administration, Writing - review & editing, Validation. **S.F. Abdullah:** Funding acquisition, Investigation. **M.N. Harif:** Methodology, Formal analysis. **H.N. Rosly:** Methodology, Formal analysis. **S.K. Tiong:** Supervision, Funding acquisition. **N. Amin:** Supervision, Funding acquisition, Resources, Validation.

Declaration of Competing Interest

The authors declare that they have no known competing financial interests or personal relationships that could have appeared to influence the work reported in this paper.

Acknowledgements

The authors wish to express the deepest appreciation to Ministry of Higher Education, Malaysia for the support through the FRGS grant code of FRGS/1/2019/STG07/UNITEN/02/1. Authors would also appreciate the substantial support for this research work from Universiti Tenaga Nasional (@UNITEN), Malaysia through BOLD2025 grant.

References

- [1] Amarasinghe M, et al. Influence of CdTe deposition temperature and window thickness on CdTe grain size and lifetime after CdCl_2 recrystallization. *IEEE J Photovoltaics* 2018;8(2):600–3.
- [2] Mathew X, Thompson GW, Singh VP, McClure JC, Velumani S, Mathews NR, et al. Development of CdTe thin films on flexible substrates—a review. *Sol Energy Mater Sol Cells* 2003;76:293–303.
- [3] Islam MA, Rahman KS, Sobayel K, Enam T, Ali AM, Zaman M, et al. Fabrication of high efficiency sputtered CdS: O/CdTe thin film solar cells from window/absorber layer growth optimization in magnetron sputtering. *Sol Energy Mater Sol Cells* 2017;172:384–93.
- [4] Seo W-O, Kim D, Kim J. Flexible CdTe/CdS solar cells on thin glass substrates. *Opt Express* 2015;23(7):A316–21.
- [5] Jung Y, et al. Growth of CdTe thin films on graphene by close-spaced sublimation method. *Appl Phys Lett* 2013;103(23):231910.
- [6] Garner S, Glaesemann S, Li X. Ultra-slim flexible glass for roll-to-roll electronic device fabrication. *Appl Phys A* 2014;116(2):403–7.
- [7] Lin Q, et al. Flexible photovoltaic technologies. *J Mater Chem C* 2014;2(7):1233–47.
- [8] Mahabaduge HP, et al. High-efficiency, flexible CdTe solar cells on ultra-thin glass substrates. *Appl Phys Lett* 2015;106(13):133501.
- [9] Rance WL, et al. 14%-efficient flexible CdTe solar cells on ultra-thin glass substrates. *Appl Phys Lett* 2014;104(14):143903.
- [10] Yang B, Ishikawa Y, Doumae Y, Miki T, Ohyama T, Isshiki M. Growth and characterization of high purity CdTe single crystals. *J Cryst Growth* 1997;172(3–4):370–5.
- [11] Isshiki, Minoru, Jifeng Wang. II-IV Semiconductors for Optoelectronics: CdS, CdSe, CdTe. In: *Springer Handbook of Electronic and Photonic Materials*. Cham: Springer; 2017, pp. 1-1.
- [12] Dharmadasa IM, Alam AE, Ojo AA, Echendu OK. Scientific complications and controversies noted in the field of CdS/CdTe thin film solar cells and the way forward for further development. *J Mater Sci: Mater Electron* 2019:1–15.
- [13] Arce-Plaza, Antonio, Fernando Sánchez-Rodríguez, Maykel Courel-Piedrahita, Osvaldo Vigil Galán, Viviana Hernández-Calderon, Sergio Ramirez-Velasco, Mauricio Ortega López, CdTe Thin Films: Deposition Techniques and Applications.

- In: *Coatings and Thin-Film Technologies*. IntechOpen; 2018.
- [14] Lee TD, Eboong AU. A review of thin film solar cell technologies and challenges. *Renew Sustain Energy Rev* 2017;70(2017):1286–97.
- [15] Britt J, Ferekides C. Thin-film CdS/CdTe solar cell with 15.8% efficiency. *Appl Phys Lett* 1993;62(22):2851–2.
- [16] Wu X, et al. 16.5%-efficient CdS/CdTe polycrystalline thin-film solar cell. In: *Proceedings of the 17th European photovoltaic solar energy conference*. Vol. 995. James & James Ltd.: London; 2001.
- [17] Dharmadasa IM, Ojo AA. Unravelling complex nature of CdS/CdTe based thin film solar cells. *J Mater Sci: Mater Electron* 2017;28(22):16598–617.
- [18] Aliyu MM, et al. Recent developments of flexible CdTe solar cells on metallic substrates: issues and prospects. *Int J Photoenergy* 2012;2012.
- [19] Reese MO, Glynn S, Kempe MD, McGott DL, Dabney MS, Barnes TM, et al. Increasing markets and decreasing package weight for high-specific-power photovoltaics. *Nat Energy* 2018;3(11):1002–12.
- [20] Willeke GP, Weber ER. *Advances in photovoltaics*. Newnes; 2013.
- [21] Krishnan S, Sanjeev G, Pattabi M, Mathew X. Effect of electron irradiation on the properties of CdTe/CdS solar cells. *Sol Energy Mater Sol Cells* 2009;93:2–5.
- [22] Ong KS, et al. Flexible polymer light emitting devices using polymer-reinforced ultrathin glass. *Thin Solid Films* 2005;477(1–2):32–7.
- [23] Auch, Mark Dai Joong, et al. Ultrathin glass for flexible OLED application. *Thin Solid Films* 2002;417(1–2):47–50.
- [24] Osedach Tim P, et al. Lateral heterojunction photodetector consisting of molecular organic and colloidal quantum dot thin films. *Appl Phys Lett* 2009;94(4):26.
- [25] Hossain MS, Rahman KS, Karim MR, Aijaz MO, Dar MA, Shar MA, et al. Impact of CdTe thin film thickness in ZnxCd1-xS/CdTe solar cell by RF sputtering. *Sol Energy* 2019;180:559–66.
- [26] Enam FMT, Rahman KS, Kamaruzzaman MI, Sobayel K, Akhtaruzzaman M, Amin N. An investigation on structural and electrical properties of close-spaced sublimation grown CdTe thin films in different growth conditions. *Chalcogenide Lett* 2017;14(4):125–31.
- [27] McCandless BE, et al. Overcoming carrier concentration limits in polycrystalline CdTe thin films with in-situ doping. *Sci Rep* 2018;8:14519.
- [28] Vyas CU, Pataniya P, Zankat CK, Pathak VM, Patel KD, Solanki GK. Transient photo-response properties of CdTe thin films synthesized by screen printing technique. *Mat Sci Semi Cond Process* 2017;71:226–31.
- [29] Luschitz J, Siepchen B, Schaffner J, Lakus-Wollny K, Haindl G, Klein A, et al. CdTe thin film solar cells: interrelation of nucleation, structure, and performance. *Thin Solid Films* 2009;517:2125–31.
- [30] Rahman Kazi Sajedur, et al. Influence of deposition time in CdTe thin film properties grown by Close-Spaced Sublimation (CSS) for photovoltaic application. *Results Phys* 2019;14:102371.
- [31] Liu, Guogen. Processing of CdS/CdTe solar cell and the growth model of CdTe thin film; 2016.
- [32] Liu, Guogen, et al. CdTe growth model by close spaced sublimation. In: *2016 IEEE 43rd Photovoltaic Specialists Conference (PVSC)*. IEEE; 2016.
- [33] Amin, Nowshad, Kazi Sajedur Rahman. Close-Spaced Sublimation (CSS): A Low-Cost, High-Yield Deposition System for Cadmium Telluride (CdTe) Thin Film Solar Cells. *Modern Technologies for Creating the Thin-film Systems and Coatings*; 2017:361.
- [34] Lv Bin, et al. The phase segregation in CdTe/CdS heterojunction and its effect on photo current of CdTe thin films solar cell. *Sol Energy* 2016;136:460–9.
- [35] Mahmood Waqar, et al. Pronounced impact of p-Type Carriers and Reduction of Bandgap in Semiconducting ZnTe Thin Films by Cu Doping for Intermediate Buffer Layer in Heterojunction Solar Cells. *Materials* 2019;12(8):1359.
- [36] Raza, Taslim M, Zishanur Rahman M, Reyaz M, Mohammad Rezaul Karim. Study of CdTe film growth by CSS on three different types of CdS coated substrates. *Mater Today: Proc* 2018;5(14):27833–27839.
- [37] Haque F, Rahman KS, Islam MA, Yusoff Y, Khan NA, Nasser AA, et al. Effects of growth temperatures on the structural and optoelectronic properties of sputtered zinc sulfide thin films for solar cell applications. *Opt Quant Electron* 2019;51(8):278.
- [38] Ohata Keiichi, Saraie Junji, Tanaka Tetsuro. Phase diagram of the CdS-CdTe pseudobinary system. *Jpn J Appl Phys* 1973;12(8):1198.
- [39] Rahman KS, Aris KA, Karim MR, Aijaz MO, Dar MA, Shar MA, et al. Impact of Cu incorporation to the CdTe thin film properties for photovoltaic application. *Chalcogenide Lett* 2017;15(5):293–306.
- [40] Oktyabrsky S. Defects Related to Zinc Blende and Wurtzite Phases in III-Nitride Heterostructures. 2001:2002–2009.
- [41] Haque F, Rahman KS, Akhtaruzzaman M, Abdullah H, Kiong TS, Amin N. Properties of sputtered ZnS thin films for photovoltaic application. *Mater Res Express* 2018;5(9):096409.
- [42] Khan NA, Rahman KS, Aris KA, Ali AM, Misran H, Akhtaruzzaman M, et al. Effect of laser annealing on thermally evaporated CdTe thin films for photovoltaic absorber application. *Sol Energy* 2018;173:1051–7.
- [43] Md Asaduzzaman, Ali Newaz Bahar, Mohammad Maksudur Rahman Bhuiyan, Md Ahsan Habib. Impacts of temperature on the performance of CdTe based thin-film solar cell. In *IOP Conference Series: Materials Science and Engineering*. IOP Publishing, 2017;225(1):012274.
- [44] Birkmire RW, Phillips JE, Shafarman WN, Hegedus SS, McCandless BE. Optimization of Processing and Modeling Issues for Thin-Film Solar Cell Devices; Annual Report, 3 February 1997-2 February 1998. No. NREL/SR-520-25845. Golden, CO (US): National Renewable Energy Lab.; 1998.
- [45] Grill R, Franc J, Hoschl P, Turkevych I, Belas E, Moravec P, et al. High-temperature defect structure of Cd- and Te-rich CdTe. *IEEE Trans Nucl Sci* 2002;49(3):1270–4.
- [46] Cruz-Campa Jose Luis, Zubia David. CdTe thin film growth model under CSS conditions. *Sol Energy Mater Sol Cells* 2009;93(1):15–8.
- [47] Potamialis C, Lisco F, Bowers JW, Walls JM. Fabrication of CdTe thin films by close space sublimation. In: *Hutchins M, Treharne R, Cole A. (Eds.) 12th Photovoltaic Science, Application and Technology Conference C, vol. 98. cc The Solar Energy Society*; 2016, p. 199–202.
- [48] Kim CC, Daraselia M, Garland JW, Sivananthan S. Temperature dependence of the optical properties of CdTe. *Phys Rev B* 1997;56(8):4786.
- [49] Gibbs Zachary M, LaLonde Aaron, Jeffrey Snyder G. Optical band gap and the Burstein-Moss effect in iodine doped PbTe using diffuse reflectance infrared Fourier transform spectroscopy. *New J Phys* 2013;15(7):075020.
- [50] Chander Subhash, Dhaka MS. Impact of thermal annealing on physical properties of vacuum evaporated polycrystalline CdTe thin films for solar cell applications. *Physica E* 2016;80:62–8.
- [51] Chander Subhash, Dhaka MS. Thermal evolution of physical properties of vacuum evaporated polycrystalline CdTe thin films for solar cells. *J Mater Sci: Mater Electron* 2016;27(11):11961–73.
- [52] Chander Subhash, Dhaka MS. CdCl₂ treatment concentration evolution of physical properties correlation with surface morphology of CdTe thin films for solar cells. *Mater Res Bull* 2018;97:128–35.
- [53] Bacaksiz E, Basol BM, Altunbaş M, Novruzov V, Yanmaz E, Nezir S. Effects of substrate temperature and post-deposition anneal on properties of evaporated cadmium telluride films. *Thin Solid Films* 2007;515(5):3079–84.
- [54] Kartopu G, Oklobia O, Turkay D, Diercks DR, Gorman BP, Barrioz Vincent, et al. Study of thin film poly-crystalline CdTe solar cells presenting high acceptor concentrations achieved by in-situ arsenic doping. *Sol Energy Mater Sol Cells* 2019;194:259–67.
- [55] Lalitha S, Sathyamoorthy R, Senthilarasu S, Subbarayan A. Influence of CdCl₂ treatment on structural and optical properties of vacuum evaporated CdTe thin films. *Sol Energy Mater Sol Cells* 2006;90(6):694–703.
- [56] Kokate AV, Asabe MR, Hankare PP, Chougule BK. Effect of annealing on properties of electrochemically deposited CdTe thin films. *J Phys Chem Solids* 2007;68:53–8.
- [57] Shaaban ER, Afify N, El-Taher A. Effect of film thickness on microstructure parameters and optical constants of CdTe thin films. *J Alloy Compd* 2009;482:400–4.
- [58] Khairnar UP, Bhavsar DS, Vaidya RU, Bhavsar GP. Optical properties of thermally evaporated cadmium telluride thin films. *Mater Chem Phys* 2003;80(2):421–7.
- [59] Spalatu Nicolae, Hiie Jaan, Valdna Vello, Caraman Mihail, Maticic Natalia, Mikli Valdek, et al. Properties of the CdCl₂ air-annealed CSS CdTe thin films. *Energy Procedia* 2014;44:85–95.
- [60] Najafi S, Safari M, Amani S, Mansouri K, Shahlaei M. Preparation, characterization and cell cytotoxicity of Pd-doped CdTe quantum dots and its application as a sensitive fluorescent nanoprobe. *J Mater Sci: Mater Electron* 2019;30(15):14233–42.
- [61] Gorji Nima E. Oxygen incorporation into CdS/CdTe thin film solar cells. *Opt Quant Electron* 2015;47(8):2445–53.